# PRELIMINARY INTERPRETATION OF ELECTRICAL SOUNDING CURVES OBTAINED ACROSS THE SNAKE RIVER PLAIN FROM BLACKFOOT TO ARCO, IDAHO

By Adel A. R. Zohdy and William D. Stanley



Prepared in cooperation with the Idaho Department of Water Administration, Atomic Energy Commission, and Bureau of Reclamation.

Open-file report

1973

## Illustrations

[Figures 1 and 18 in pocket; figures 2-17 follow text]

# SOUNDING CURVES OBTAINED ACROSS THE SNAKE RIVER PLAIN FROM BLACKFOOT TO ARCO, IDAHO

By Adel A. R. Zohdy and William D. Stanley

During August 1971, the U.S. Geological Survey made 38 d-c resistivity soundings along a profile from Blackfoot to Arco, Idaho. The purpose of the survey was threefold: 1) determine the thickness of the basalt flows of the Snake River Group, which form the main aquifer in the Snake River Plain, 2) determine the nature of the materials underlying the basalt, and 3) estimate the depth to the high-resistivity basement rocks beneath the Snake River Plain.

The locations of the VES (vertical electrical sounding) stations are shown on figure 1. All the soundings were made with the Schlumberger AMNB array with electrode spacings (AB/2) often expanded to 12,000 feet. VES 8, VES 12, VES 24, VES 29, and VES 38 were expanded to larger electrode spacings (up to 58,000 feet) using bilaterial equatorial arrays, and VES 19 was expanded to 68,600 feet using a unilateral equatorial array. VES 15 was expanded to 68,600 feet using a bilateral polar array; and VES 21 was expanded to 32,000 feet using a unilateral polar array. The observed VES curves are shown in figures 2 through 17. The apparent resistivity is plotted on the ordinate axis and the Schlumberger electrode spacing (AB/2 = half distance between current electrodes), the equatorial spacing ($\overline{R}$ = distance from one current electrode to center of potential dipole), and the polar dipole spacing (r = distance between centers of current and potential dipoles) are plotted on the abscissa axis.

Figure 18 shows the geoelectric section obtained from the preliminary interpretation of the VES curves using curve matching procedures (Kalenov, 1957; Orellana and Mooney, 1966). On this section there are five geoelectrical units. The 1,000-3,000 ohm-meter layer is interpreted as dry basalt. The 300-600 ohm-meter layer is interpreted as basalt saturated with fresh water. The 100-200 ohm-meter layer is interpreted as basalt flows intercalated with clayey sedimentary rocks. The 20-40 ohm-meter layer is interpreted as sedimentary rocks and/or rhyolitic ash-flow tuff. The geoelectric basement at the bottom of the section has a high resistivity, about 500 ohm-meters or more, and it may represent Paleozoic rocks.

The deep structural trough on the southeastern part of the profile is filled with materials having a resistivity of about 40 ohm-meters. The depth to the electric basement in that structure is estimated to be at least 20,000 feet. Whether this structural trough represents a caldera or a graben cannot be determined from the available VES data.

## References

Kalenov, E.N., 1957, Interpretation of vertical electrical sounding curves [in Russian]: Moscow, Gostoptelkhizdat, 471 p.

Orellana, Ernesto, and Mooney, H. M., 1966, Master tables and curves for vertical electrical sounding over layered structures: Madrid, Interciencia.

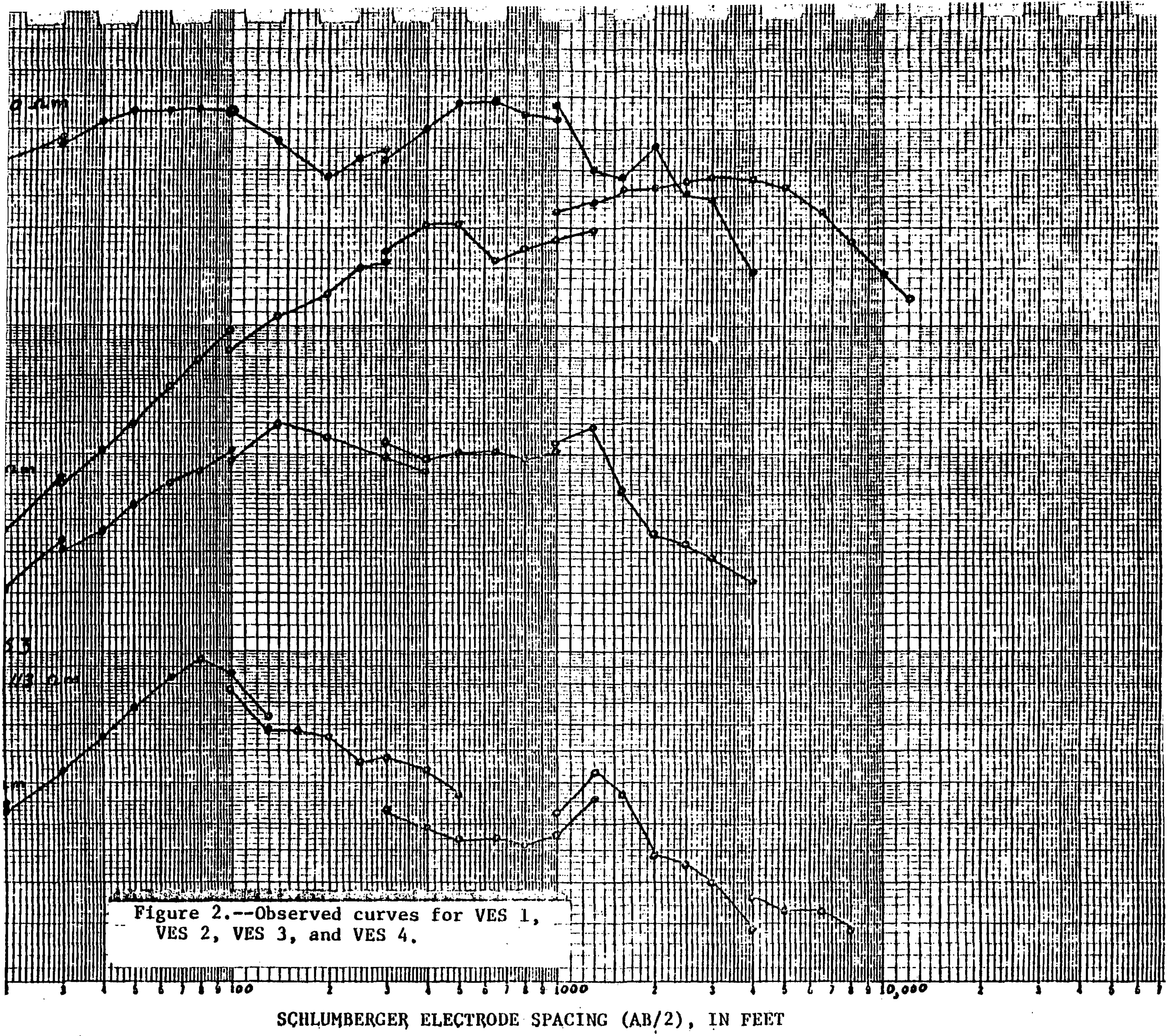


Figure 2.--Observed curves for VES 1, VES 2, VES 3, and VES 4.

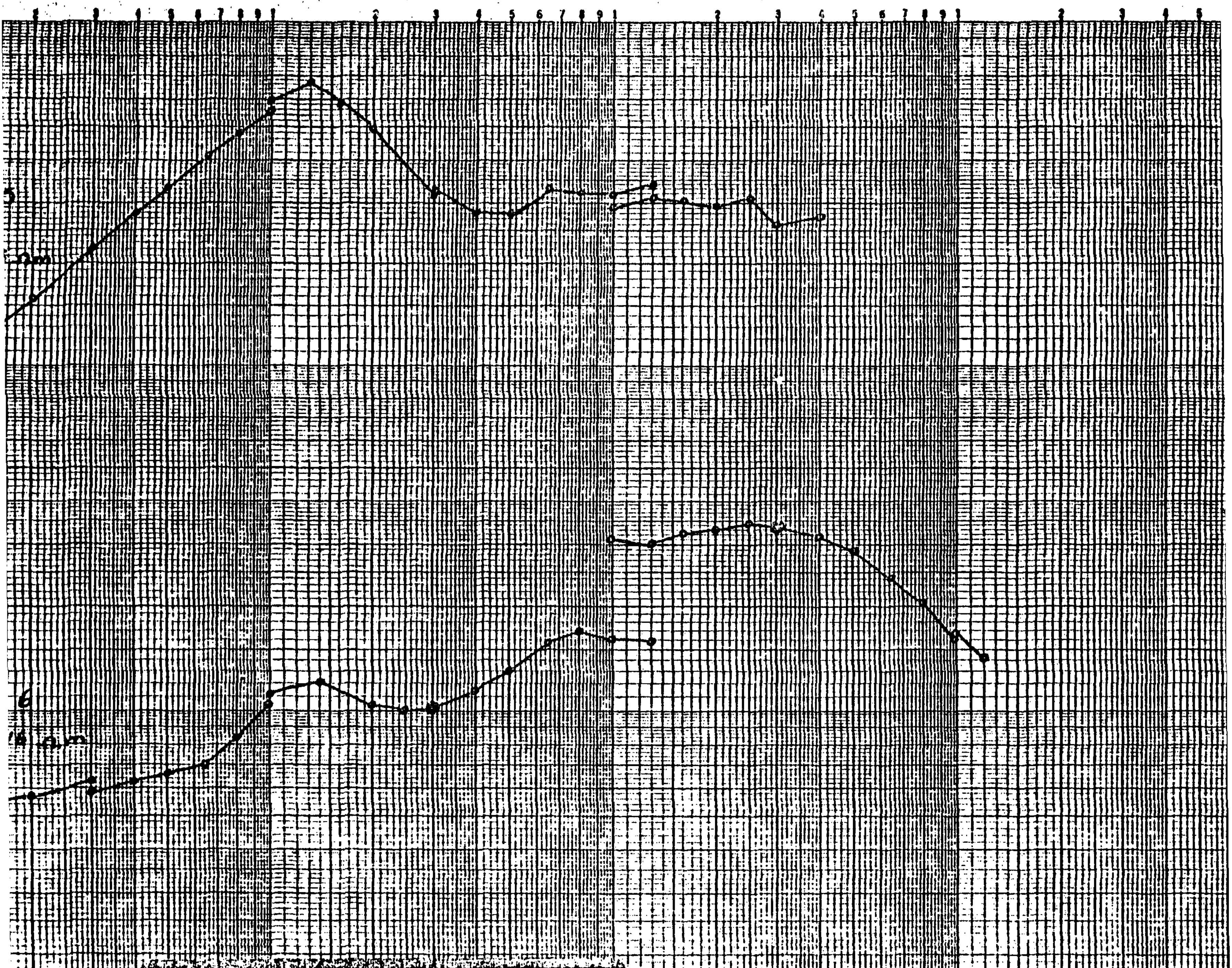


Figure 3.--Observed curves for VES 5 and VES 6.

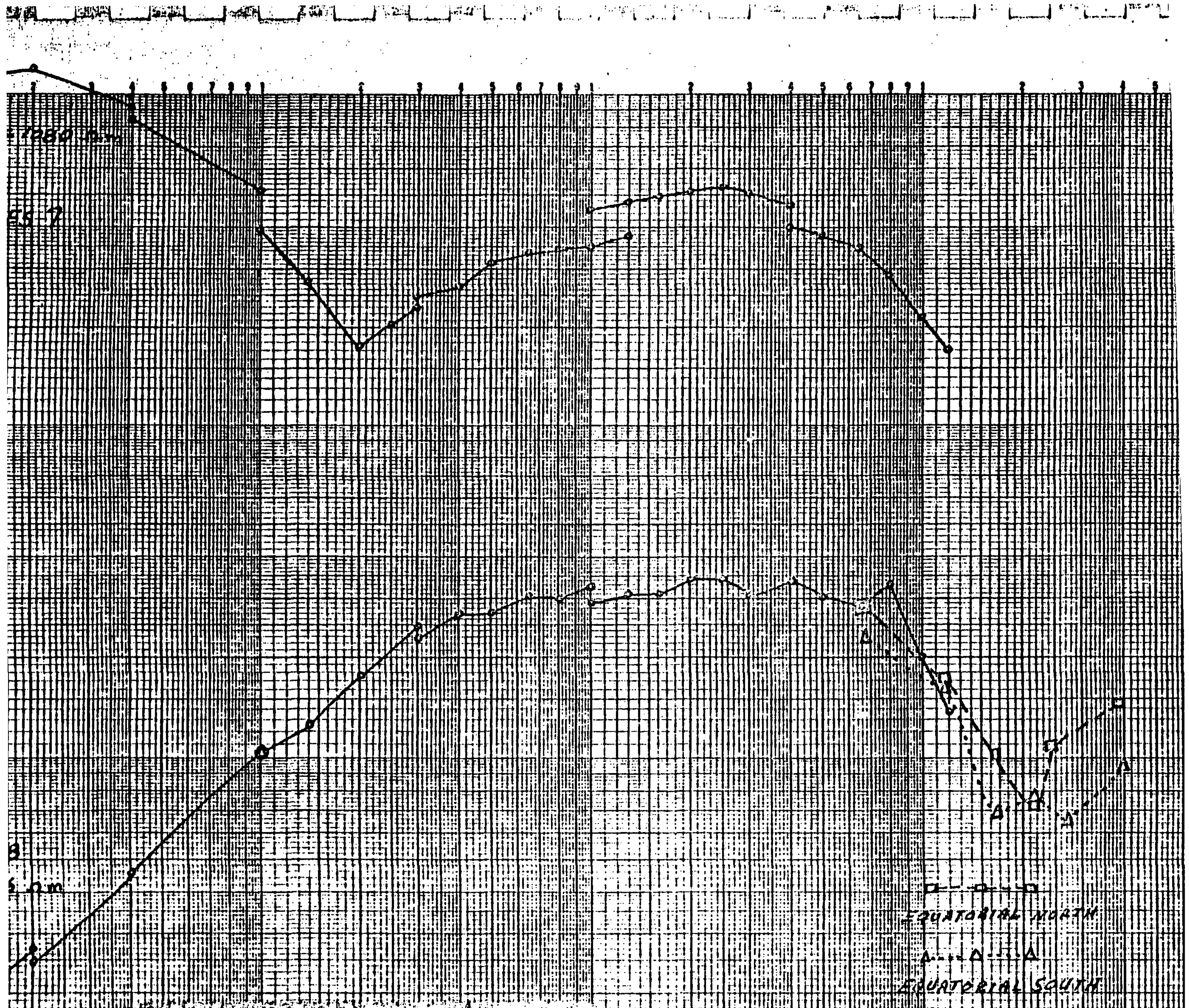


Figure 4.--Observed curves for VES 7 and VES 8.

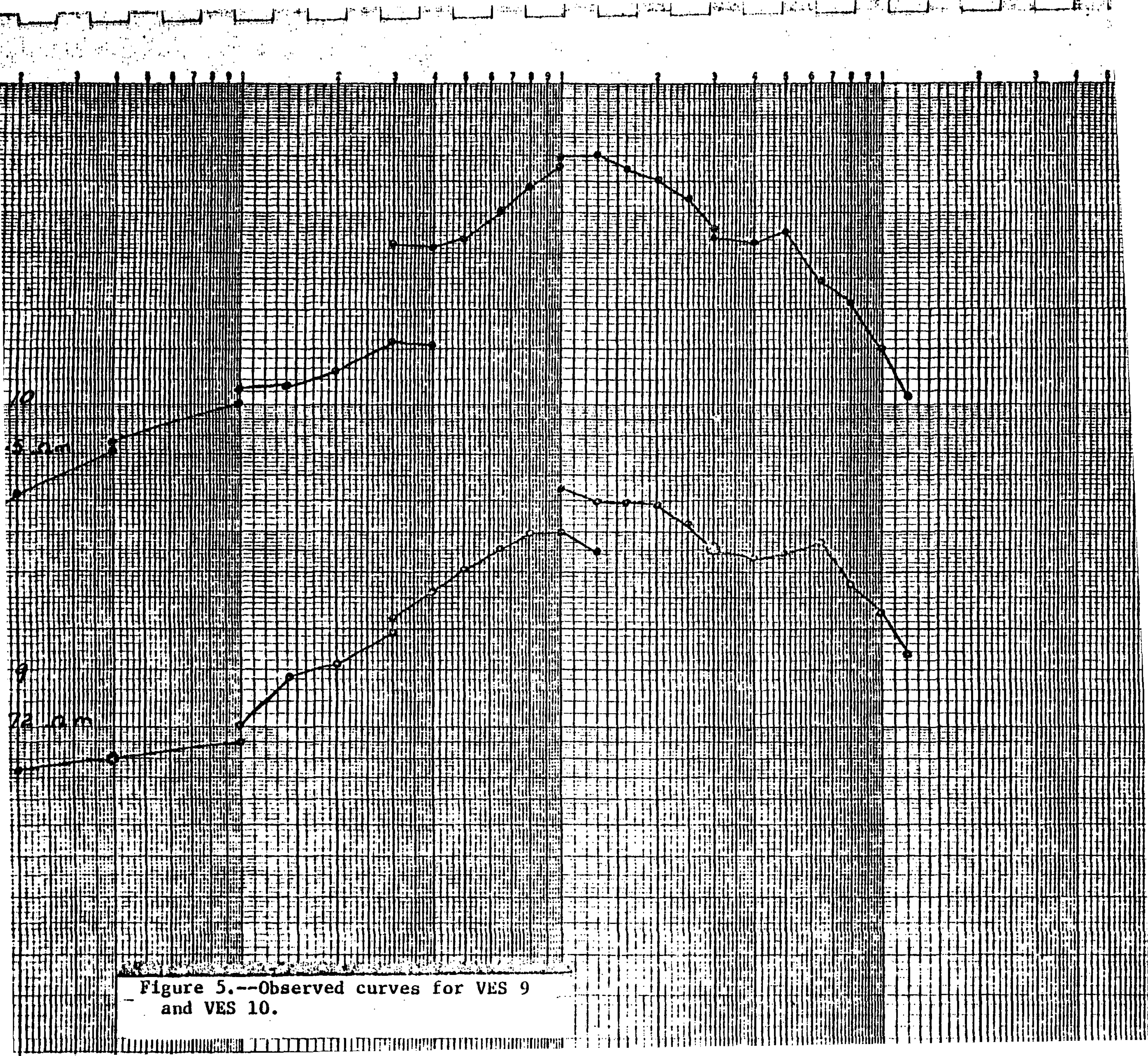


Figure 5.--Observed curves for VES 9 and VES 10.

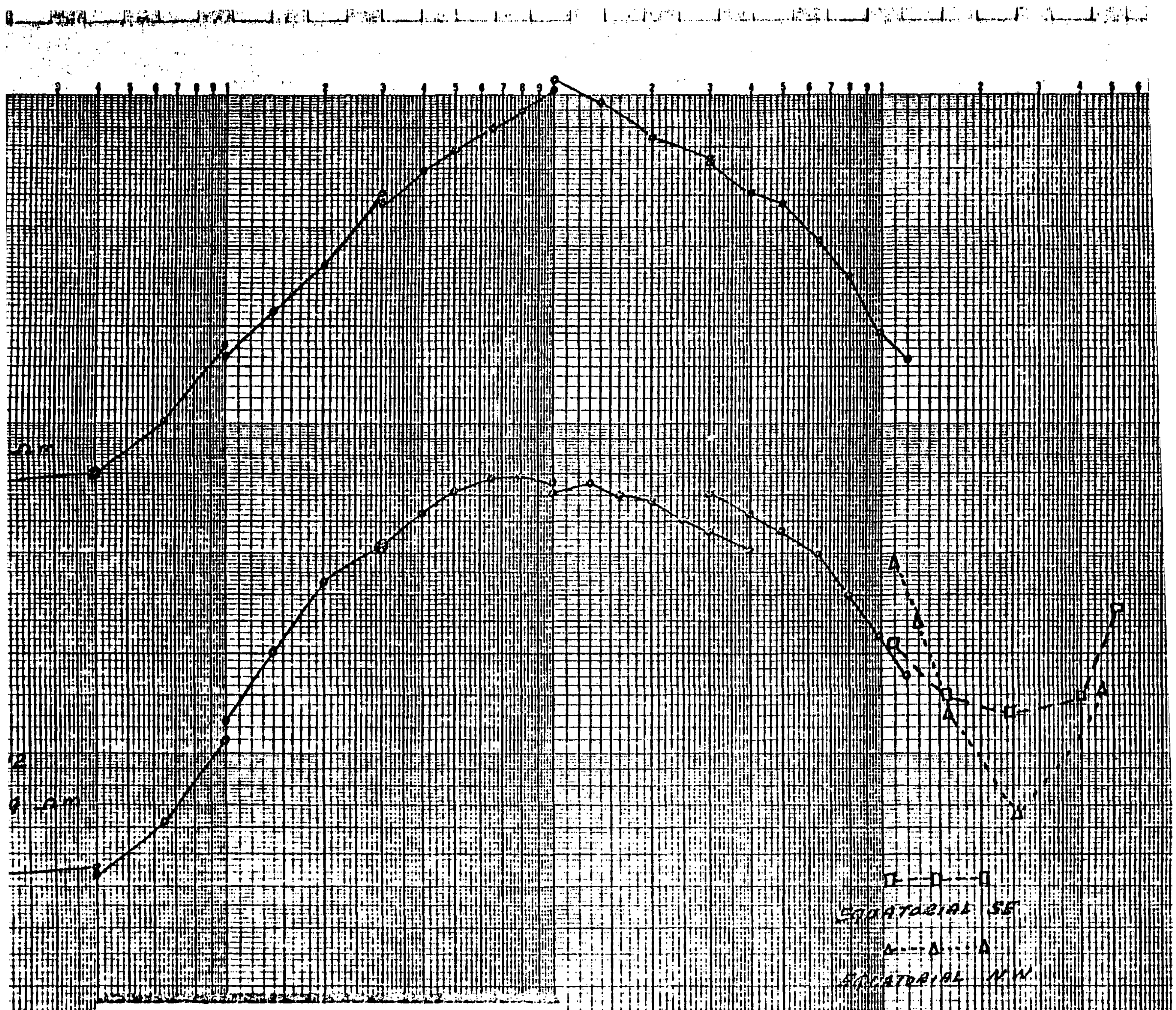


Figure 6.--Observed curves for VES 11 and VES 12.

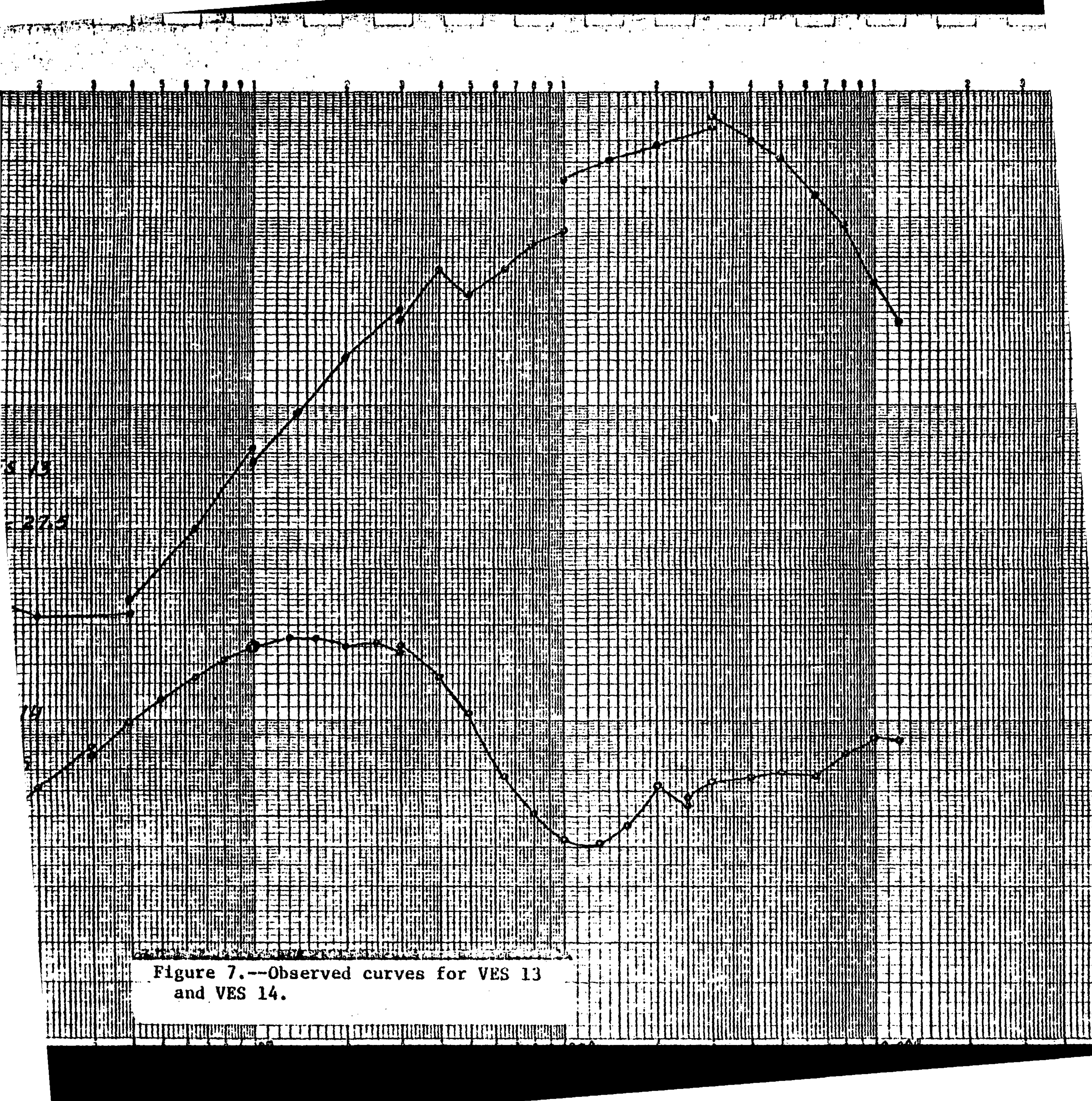


Figure 7.--Observed curves for VES 13 and VES 14.

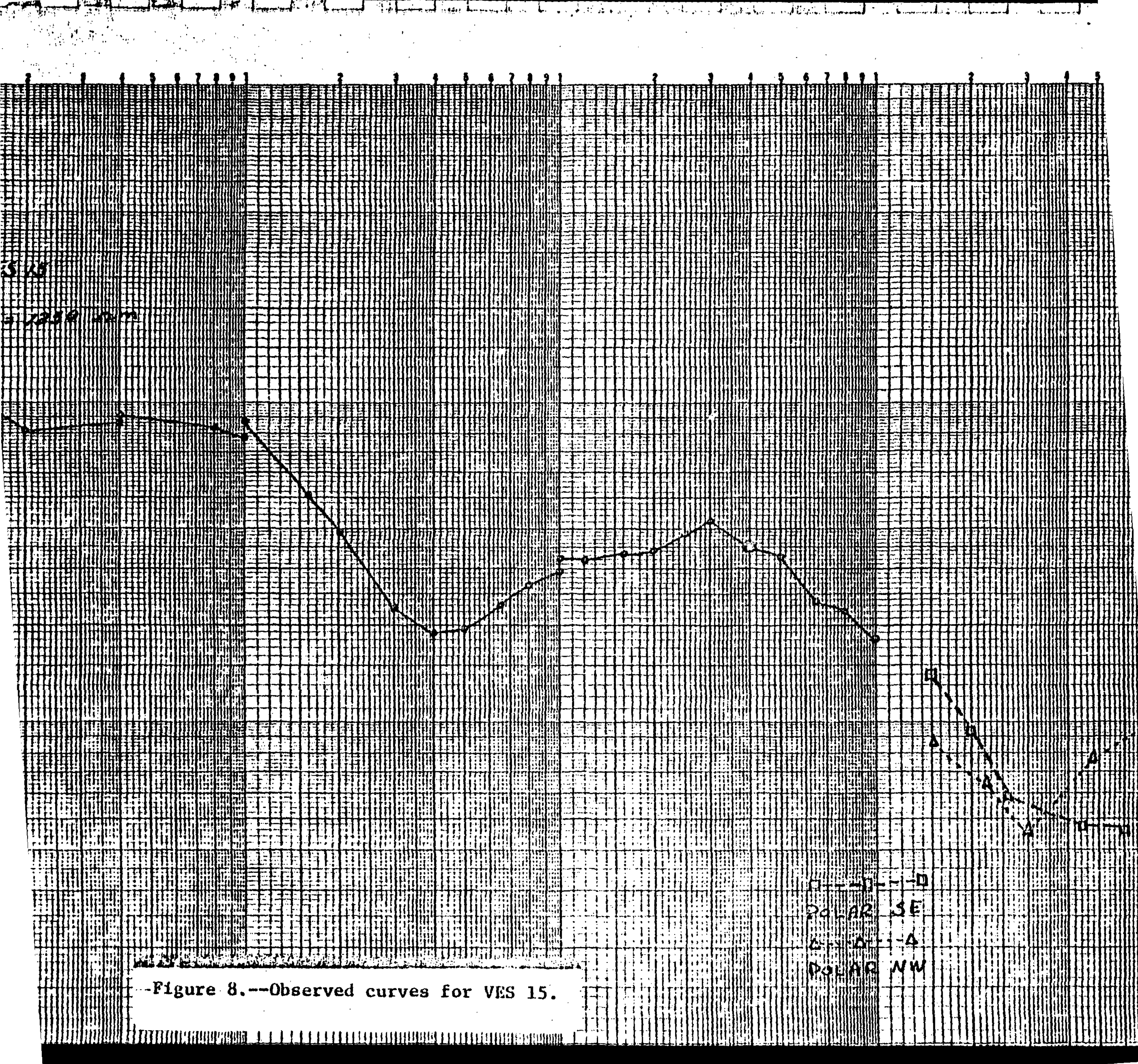


Figure 8.--Observed curves for VES 15.

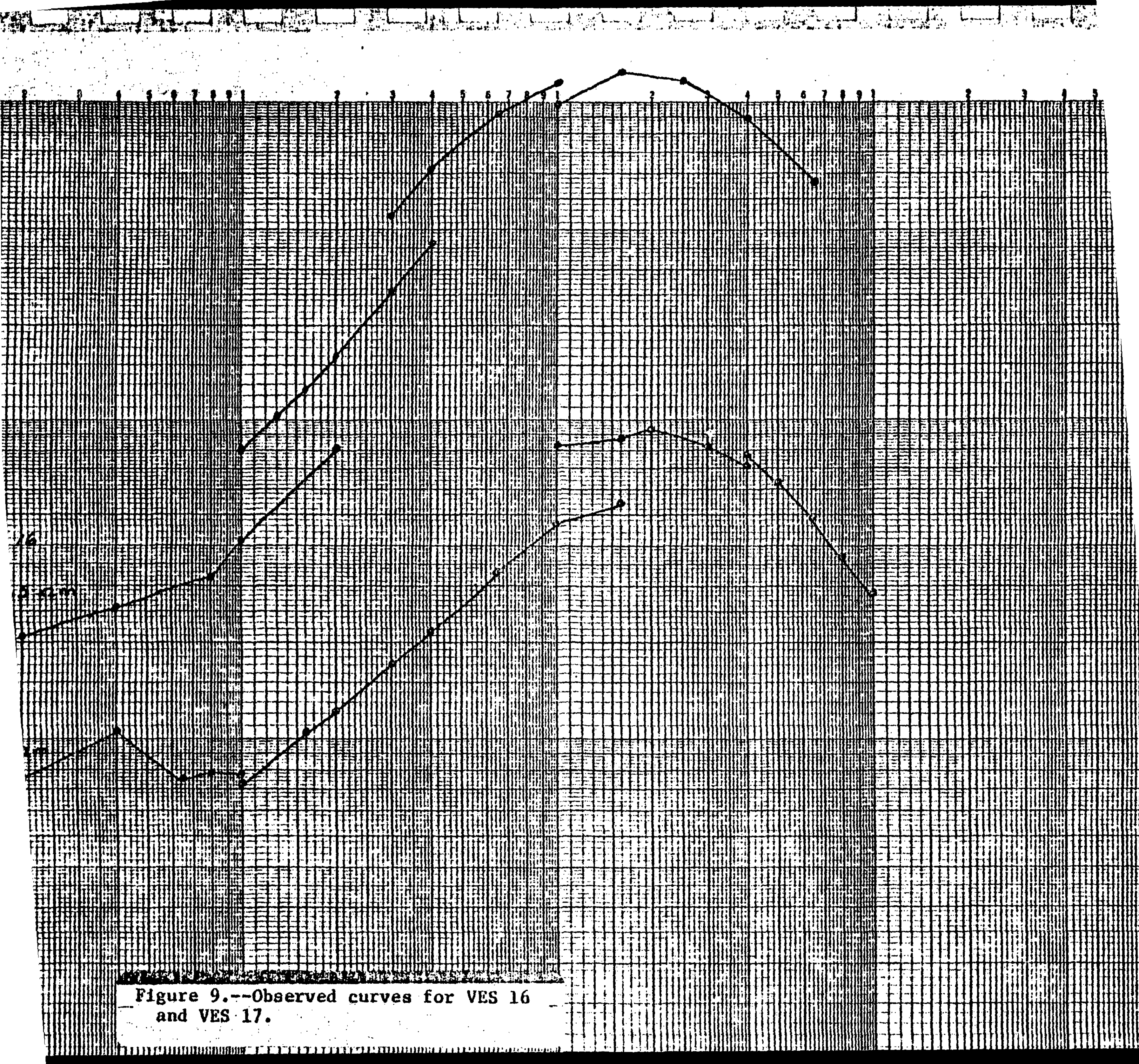

Figure 9.--Observed curves for VES 16 and VES 17.

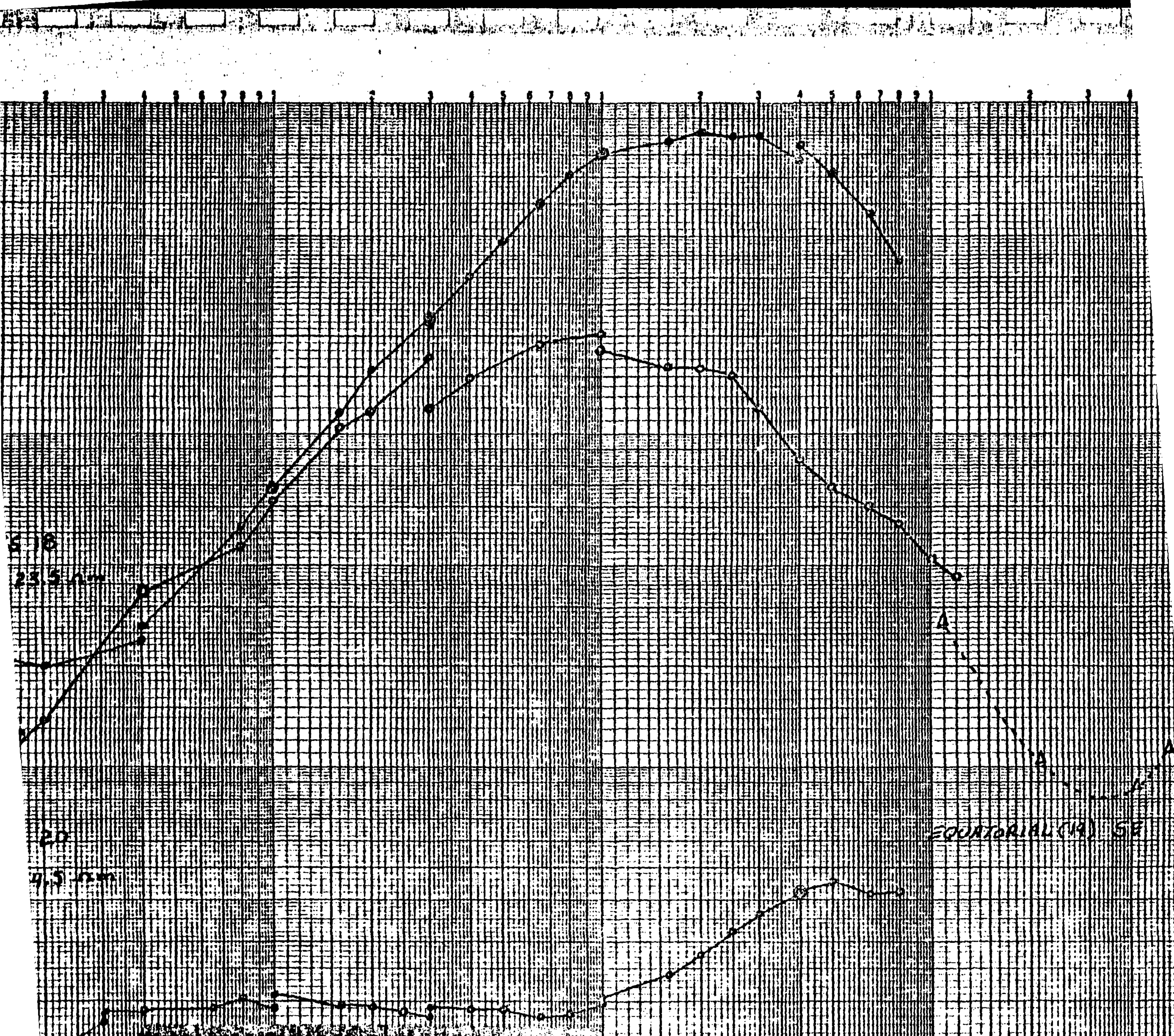


Figure 10.--Observed curves for VES 18, VES 19, and VES 20.

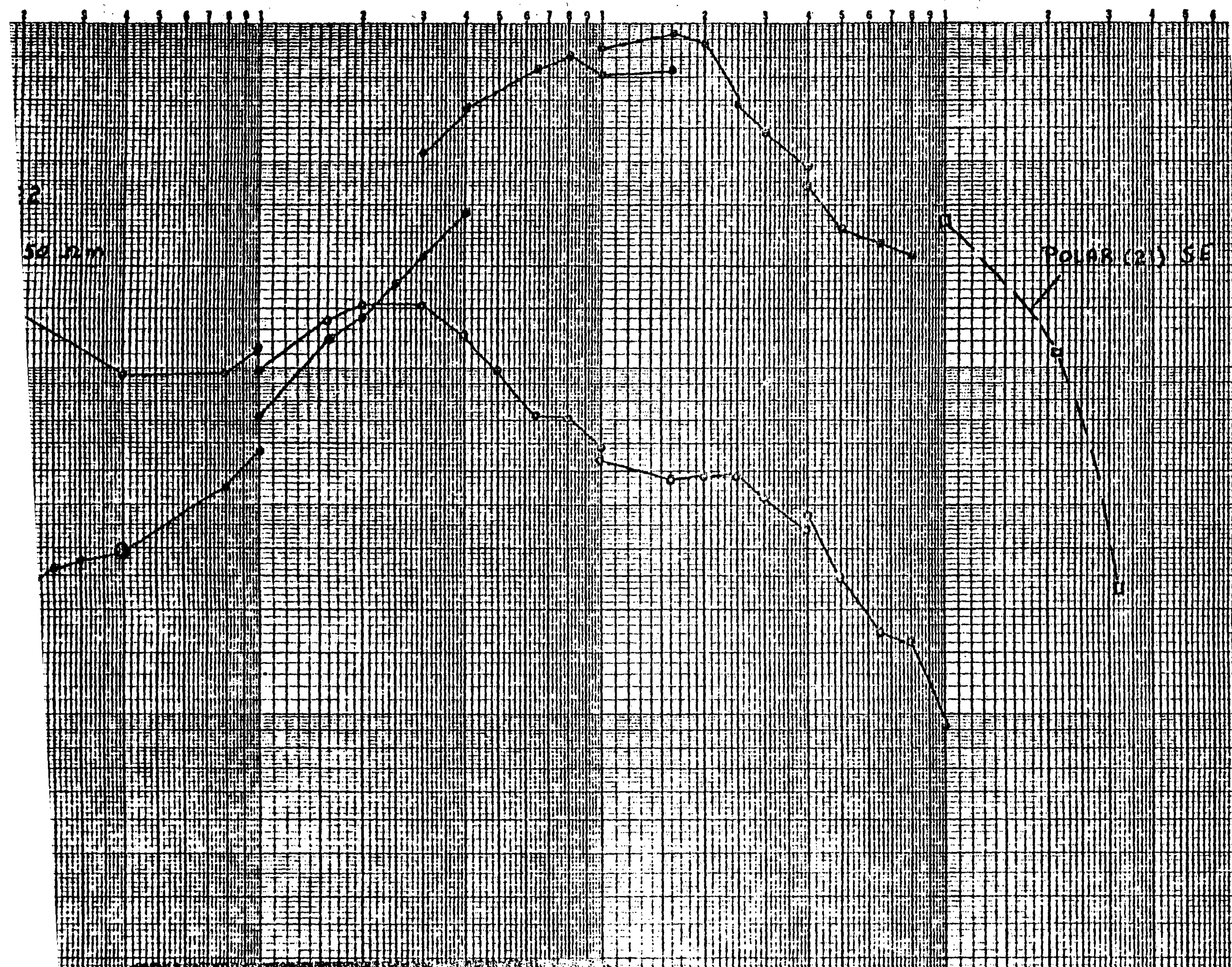


Figure 11.--Observed curves for VES 21 and VES 22.

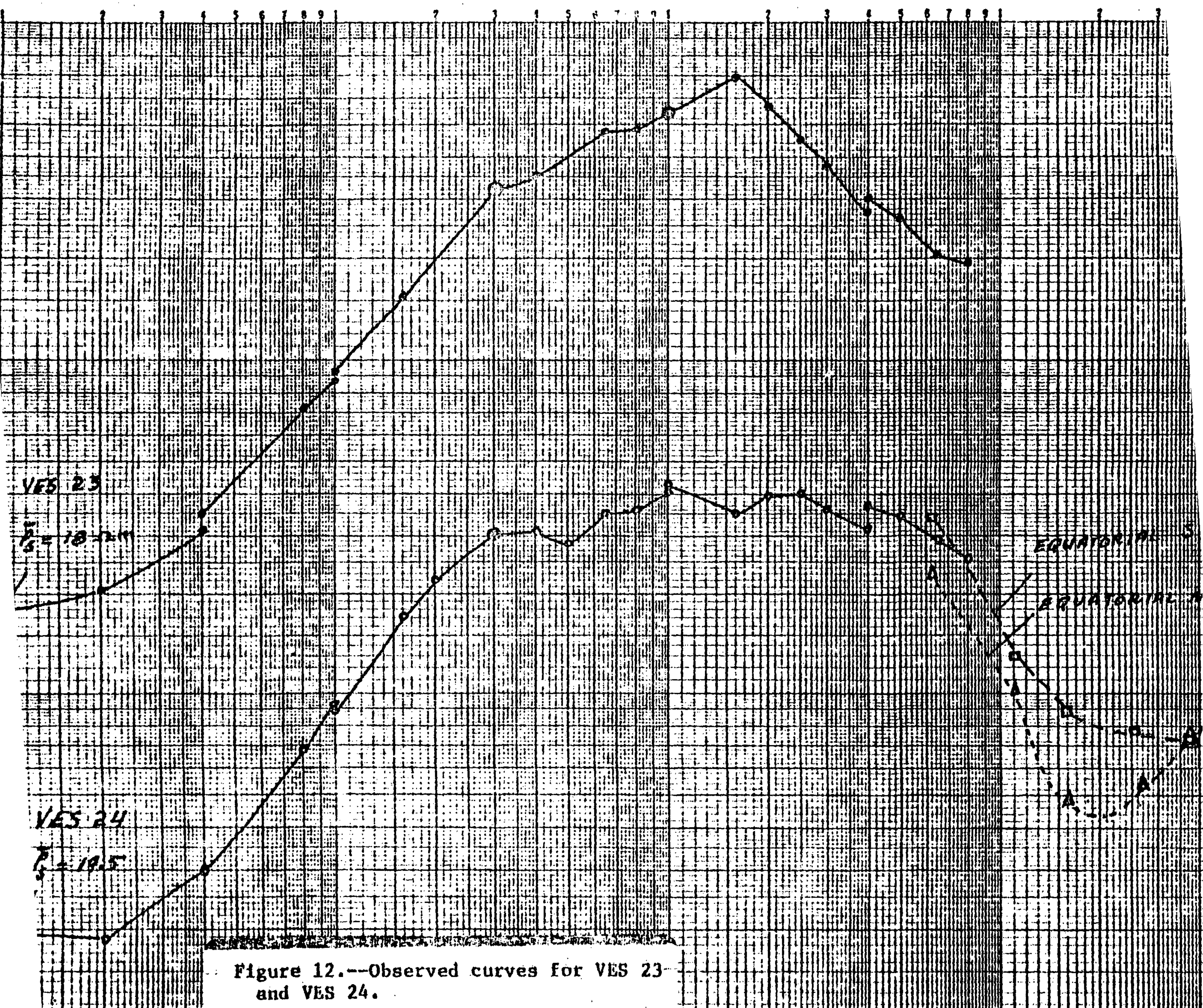


Figure 12.--Observed curves for VES 23 and VES 24.

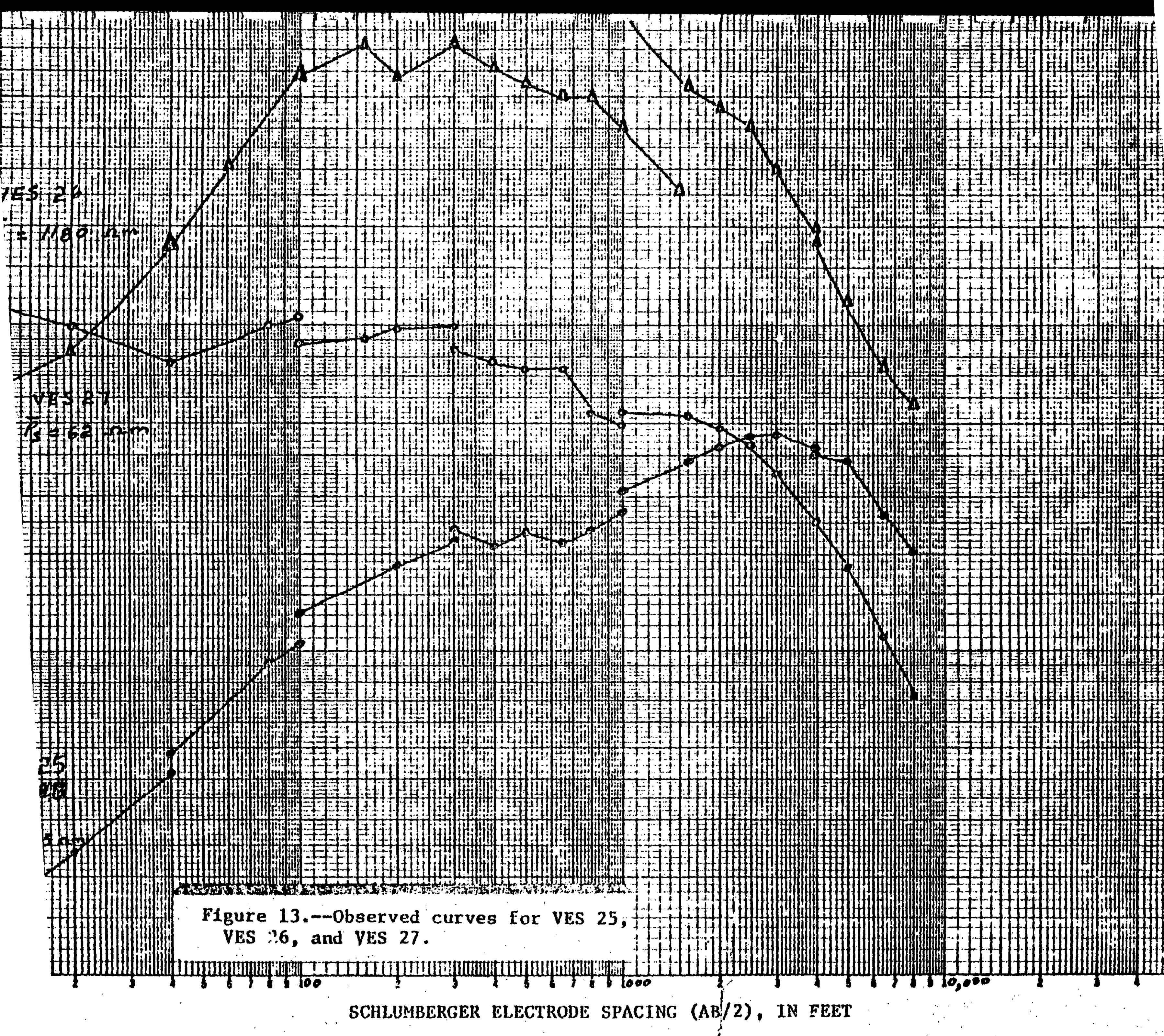


Figure 13.--Observed curves for VES 25, VES 26, and VES 27.

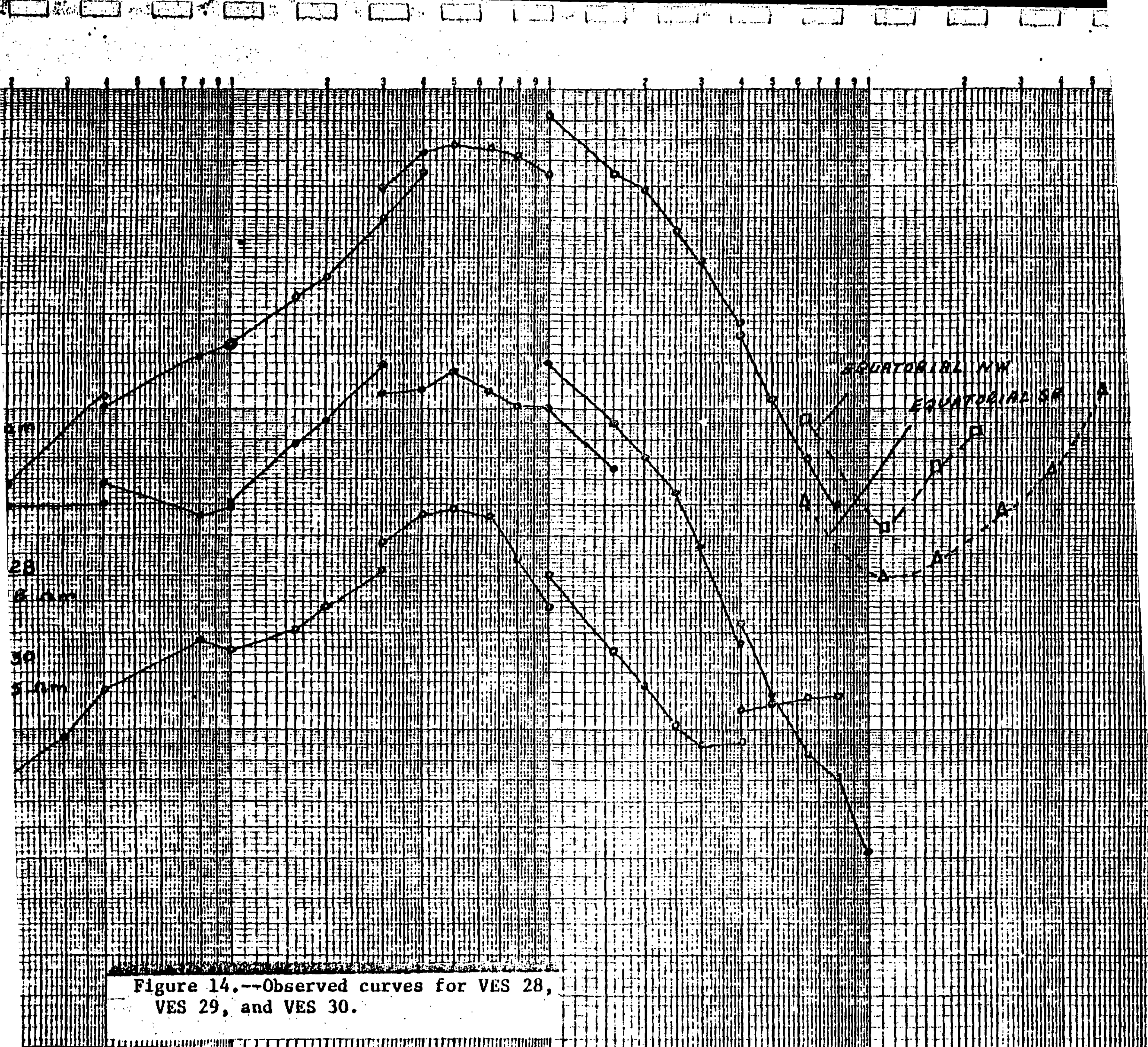


Figure 14.--Observed curves for VES 28, VES 29, and VES 30.

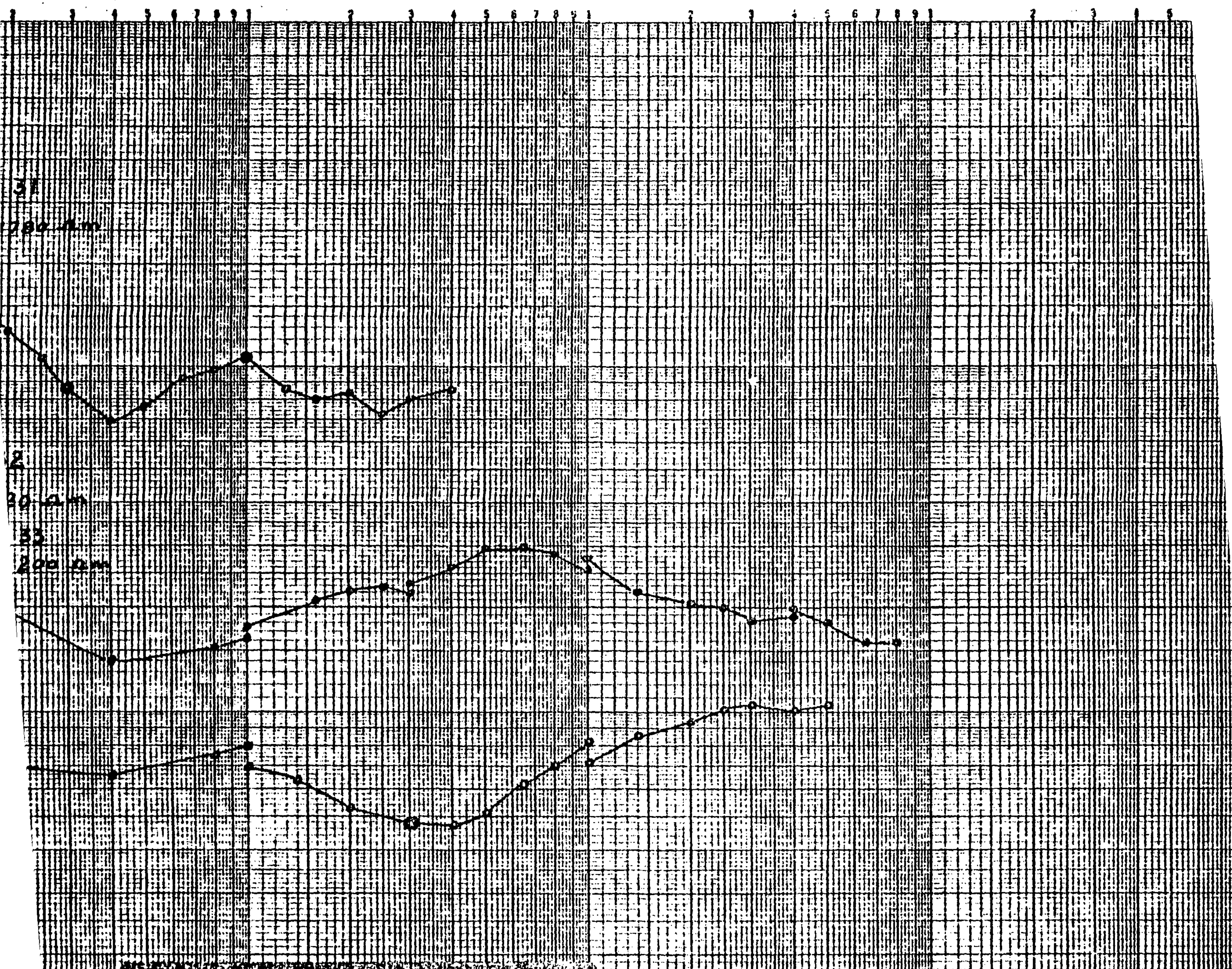

Figure 15.--Observed curves for VES 31, VES 32, and VES 33.

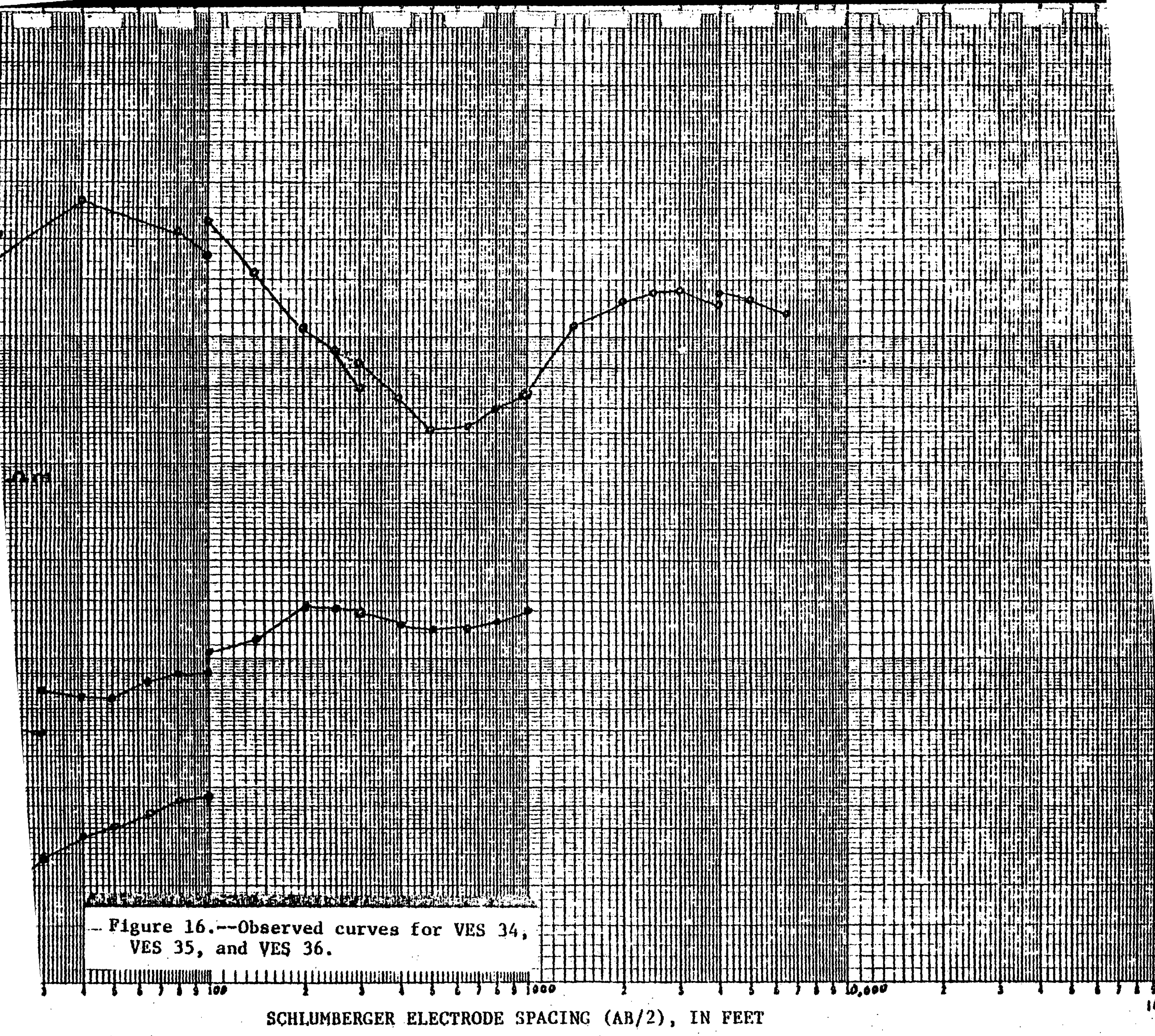


Figure 16.--Observed curves for VES 34, VES 35, and VES 36.

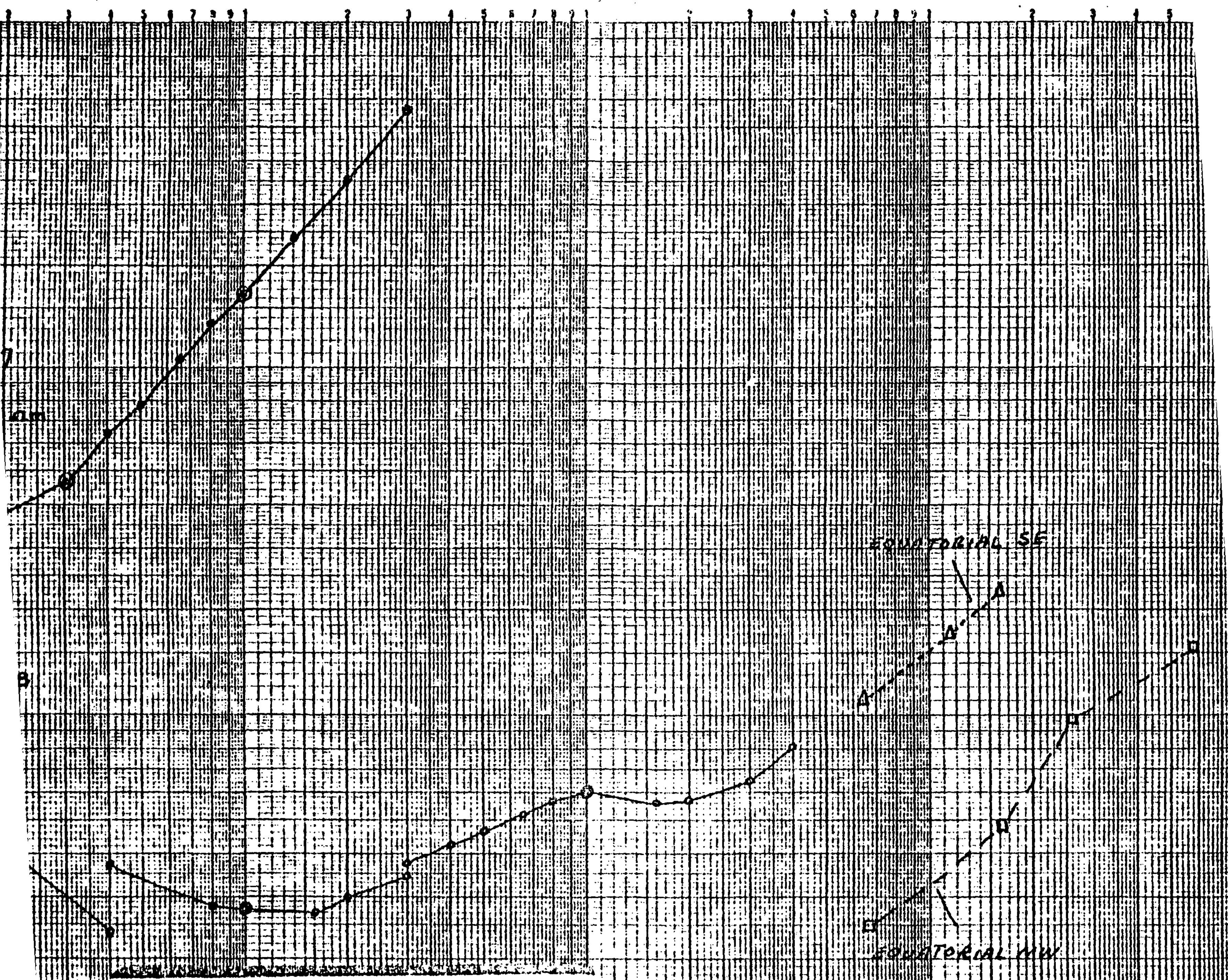


Figure 17.--Observed curves for VES 37 and VES 38.